MITSUBISHI ELECTRIC RESEARCH LABORATORIES
http://www.merl.com

Vehicle Yaw Dynamics Control by Torque-based Assist Systems Enforcing Driver's Steering Feel Constraints

Zafeiropoulos, S.; Di Cairano, S.

TR2013-040 June 2013

Abstract

We investigate the control of torque-based steering assist systems for improving yaw rate tracking and vehicle stabilization. As opposed to active front steering systems based on harmonic motors, torque-based steering assist systems are mechanically coupled with the driver. Thus, besides standard vehicle and actuators constraints, specific constraints related to the driver-actuator interaction need to be enforced. These constraints can be formulated to achieve a multiplicity of goals, including avoiding excessive strain in the driver's arms, and preserving the driver's "feel for the road". In order to achieve high control performance and constraints satisfaction, we implement controllers based on linear and switched model predictive control, where different types of driver's steering feel constraints are enforced. The different controllers are evaluated in simulation maneuvers to analyze their capabilities and the impact of the constraints in terms of vehicle cornering, stabilization, and driver's steering feel.

American Control Conference (ACC)

Vehicle Yaw Dynamics Control by Torque-based Assist Systems Enforcing Driver's Steering Feel Constraints

Spyridon Zafeiropoulos, Stefano Di Cairano

***Abstract*— We investigate the control of torque-based steering assist systems for improving yaw rate tracking and vehicle stabilization. As opposed to active front steering systems based on harmonic motors, torque-based steering assist systems are mechanically coupled with the driver. Thus, besides standard vehicle and actuators constraints, specific constraints related to the driver-actuator interaction need to be enforced. These constraints can be formulated to achieve a multiplicity of goals, including avoiding excessive strain in the driver's arms, and preserving the driver's "feel for the road". In order to achieve high control performance and constraints satisfaction, we implement controllers based on linear and switched model predictive control, where different types of driver's steering feel constraints are enforced. The different controllers are evaluated in simulation maneuvers to analyze their capabilities and the impact of the constraints in terms of vehicle cornering, stabilization, and driver's steering feel.**

I. Introduction

In the pursuit to achieve zero accidents on the road, several active safety systems for vehicle stability control are being investigated. Electronic stability control (ESC) [1] exploits differential braking, and has been proved effective in reducing single vehicle accidents [2]. Although not as effective as ESC in stabilization, steering-based driver assist systems are capable of improving both cornering performance and vehicle stability, and are less intrusive for the driver. Among steering assist systems, active font steering (AFS) [3], which modifies the relation between the steering wheel angle (SWA) and the tire road wheel angles (RWA) at the front tires, has been extensively investigated for vehicle control, also in combination with ESC [3]–[6].

In this paper we consider vehicle cornering and stability control exploiting a *torque-based* steering assist system [7]. These systems are already present in several production vehicles via, for instance, Electric Power Steering (EPS), although not yet used for stability control. The torque applied by the assist system affects the torque felt by the driver through the steering wheel, the so called driver steering (torque) feel. The driver steering feel is one of the primary ways drivers sense the road conditions and the current vehicle dynamics behavior [8], and hence it must be preserved.

Preservation of the steering feel has been investigated before, see e.g., [9]–[11]. Here, we combine vehicle cornering and stability control with steering feel control by accounting for the effects of the steering assist system on the strain torque exerted on the driver. In order to achieve this, we develop model predictive control strategies (MPC) [12] based on a model of the vehicle, the steering system, and the driver, that aims at optimizing yaw rate tracking, while enforcing stability via slip angle constraints, and mechanical and driver's steering torque feel constraints on the torque actuator. These constraints limit the capabilities of the torque-assist system hence imposing a fundamental trade-off between vehicle control capabilities and driver feels.

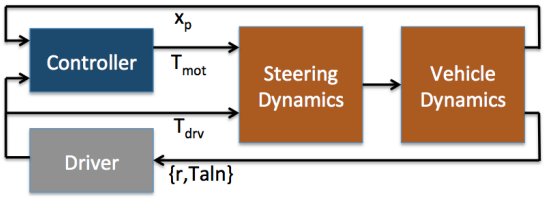

Fig. 1: Schematics of the subsystems and MPC controller.

The paper is structured as follows. In Section II we formulate the steering and vehicle dynamics with respect to the tire sideslip angles, and in Section III we introduce a model for the driver and its interaction with the vehicle. In Section IV we introduce vehicle stability constraints and constraints on the interaction between driver and steering-assist system. In Section V we develop linear MPC and switched MPC (sMPC) strategies to trade-off between the vehicle dynamics performance and the driver torque feel. In Section VI we present simulation results for different types of constraints in a specific maneuver. Conclusions and future developments are summarized in Section VII.

Notation: for a discrete-time signal with sampling period t_s, $x(k)$ is the value of x at time kt_s, and $a(h|k)$ is the predicted value of $a(k+h)$ basing on data at time k. Inequalities between vectors are intended componentwise. We indicate a matrix of appropriate dimensions entirely composed of zeros by 0.

II. Vehicle Model

The system we consider is composed of three subsystems, vehicle (chassis), steering system, and driver, that are connected as shown in Figure 1.

A. Vehicle dynamics

We focus on normal driving turning maneuvers, where the vehicle dynamics can be conveniently approximated by the bicycle model [13] (see Figure 2). The approximated model

Spyridon Zafeiropoulos is a graduate student at the D. Guggenheim School of Aerospace Engineering, Georgia Inst. Technology, Atlanta, GA, spyros.zaf@gatech.edu

S. Di Cairano is with Mitsubishi Electric Research Laboratories, Cambridge, MA, dicairano@ieee.org.

Spyridon Zafeiropoulos did this research while at MERL.

has reduced complexity with respect to a four-wheel vehicle model, while still capturing the relevant dynamics.

We consider a reference frame that moves with the vehicle. The frame origin is at the vehicle center of mass, with the x-axis along the longitudinal vehicle direction pointing forward, the y-axis pointing to the left side of the vehicle, and the z-axis pointing upwards. The tire sideslip angles, or simply slip angles (the angles between tire directions and velocity vectors at the tires), are denoted by α_f [rad] and α_r [rad] for front and rear tires, respectively. Since we are interested only in normal driving, where the vehicle needs to remain in the stable region, we approximate the tire forces as linear functions of the slip angles (see lower left corner of Figure 2)

$$F_j(\alpha_j) = c_j \alpha_j, \tag{1}$$

where $j \in \{f, r\}$, $j = r$ for the rear tires, and $j = f$ for the front tires, and c_j [N/rad] are identified from experimental data or more detailed models [14]. The approximation in (1) is considered valid for $\alpha_j \leq p_j$, where p_j [rad] is the tire *saturation angle*.

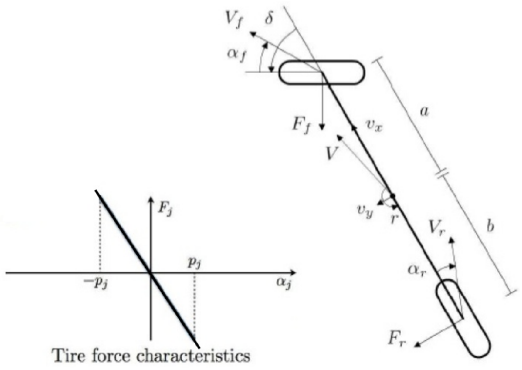

Fig. 2: Schematics of the bicycle model of the vehicle, and qualitative approximation of the sideslip angle-tire force relation.

By following a procedure similar to [15], assuming the longitudinal velocity at the wheels being constant and equal to the one at the center of mass v_x [m/s], and the tire sideslip angles and the steering angle (δ [rad]) being small, the yaw rate r [rad/s] is expressed by

$$r = \frac{v_x}{a+b}\left(\alpha_f - \alpha_r + \frac{\delta}{G_g}\right), \tag{2}$$

and the vehicle dynamics are described by

$$\dot{\alpha}_f = \frac{F_f+F_r}{m v_x} - \frac{v_x}{a+b}\left(\alpha_f - \alpha_r + \frac{\delta}{G_g}\right) + \frac{a}{v_x I_z}(aF_f - bF_r) - \frac{\varphi}{G_g} \tag{3a}$$

$$\dot{\alpha}_r = \frac{F_f+F_r}{m v_x} - \frac{v_x}{a+b}\left(\alpha_f - \alpha_r + \frac{\delta}{G_g}\right) - \frac{b}{v_x I_z}(aF_f - bF_r) \tag{3b}$$

$$\dot{\delta} = \varphi, \tag{3c}$$

where m [kg] is the vehicle mass, a [m] and b [m] are the distances of the front and rear wheel axes from the vehicle center of mass, I_z [kgm^2] is the vehicle moment of inertia with respect to the center of mass, φ [rad/s] is the steering angular rate, and G_g is the steering column reduction gear. Therefore, the continuous-time dynamics (1), (2), (3) are represented by the linear system

$$\dot{x}_v(t) = A^c x_v(t) + B^c u_v(t) \tag{4a}$$

$$y_v(t) = C^c x_v(t). \tag{4b}$$

In (4) the state vector is $x_v = [\alpha_f \ \alpha_r \ \delta]'$, the input vector is $u_v = \varphi$, and the output vector is $y_v = r$.

B. Steering dynamics

The steering dynamics describe the rotational dynamics of the steering column due to the torques applied by the driver, the steering assist system and the road-tire interaction. They are expressed by

$$J\dot{\varphi} = (T_{\rm drv} + T_{\rm mot} - T_{\rm aln}) - \beta\varphi, \tag{5}$$

where β [Nm s/rad] is the friction coefficient of the steering column, J [kgm^2] is the column moment of inertia, and $T_{\rm drv}$ [Nm], $T_{\rm mot}$ [Nm], and $T_{\rm aln}$ [Nm] are the torques generated by driver, steering assist system motor, and road-tire interaction (the so called alignment torque) reported at the steering wheel, respectively. Here, the alignment torque is modeled by a linear function of the front tire sideslip angle

$$T_{\rm aln} = K_\alpha \alpha_f. \tag{6}$$

Even though (6) is an approximation, it can be seen in [16] and [8] to be appropriate in certain operating ranges and conditions.

III. Driver-Steering Interaction

In this work we control the vehicle dynamics by a torque-based steering assist system while accounting for the driver's feel through the steering wheel, where we define as *driver's steering torque feel* (hereafter simply driver's feel) the torque that is felt by the driver through the steering wheel. Therefore, we model the driver, the driver's feel, and how the torque-based steering-assist system affects the driver's feel.

A. Driver model

We consider a feedforward plus feedback driver model

$$T_{\rm drv} = T^{\rm fb}_{\rm drv} + F^{\rm ff}_{\rm drv}. \tag{7}$$

The feedforward term compensates for the alignment moment, $F^{\rm ff}_{\rm drv} = T_{\rm aln}$, while the feedback term enforces tracking of a desired yaw rate $r_{\rm des}$,

$$T^{\rm fb}_{\rm drv} = -K_{\rm p}(r - r_{\rm des}). \tag{8}$$

By (7), (8), we model the driver as a proportional controller with gain K_p from the yaw rate tracking error, and with a feedforward term that compensates for the alignment torque.

B. Assist system impact on the feel for the road

The notion of driver's steering feel was introduced in [8] as related to the *feel for the road*, namely the alignment torque $T_{\rm aln}$ exerted by the road on the steering system. In this work we model how a torque-based steering assist system affects

the sensed steering torque, and how to control such system accounting for the driver feel. The steering assist system, is a torque generating motor placed on the steering column and has direct connection with both the driver and the wheels. Therefore, the steering torque felt by the driver is

$$T_{\rm fb} = T_{\rm aln} - T_{\rm mot}. \tag{9}$$

In the case of absence of motor torque, the felt torque is equal to the alignment torque. But, whenever active, the motor modifies that. For instance, when $T_{\rm fb} < T_{\rm aln}$, the driver feels the steering wheel "lighter". Indeed, if $T_{\rm fb} > T_{\rm aln}$, the driver feels the steering wheel "heavier".

In order to obtain both, vehicle performance and vehicle drivability and comfort, we need to account for the impact of the motor on the driver's feel. Hence, the steering assist system needs to act as a driving aid while satisfying constraints on $T_{\rm fb}$. Note that the feel torque is also the strain torque in the driver's arms holding the steering wheel, $T_{\rm str}$, caused by the torques applied to the steering column by the steering assist motor and the road.

IV. Vehicle and Driver Constraints

Controlling the vehicle dynamics and driver's feel imposes mechanical constraints on the steering assist actuator, vehicle stability constraints, and driver's feel constraints. The mechanical constraints enforce the design and physical limitations of the torque actuator in terms of output torque generated by the motor, and of output torque rate,

$$T_{\rm mot}^{\rm min} \le T_{\rm mot} \le T_{\rm mot}^{\rm max}, \tag{10a}$$
$$\dot{T}_{\rm mot}^{\rm min} \le \dot{T}_{\rm mot} \le \dot{T}_{\rm mot}^{\rm max}. \tag{10b}$$

The vehicle stability constraints are enforced on the slip angles for avoiding stability losses [5], [15], and to keep the vehicle state trajectory in the region where the tire forces approximation (1) is accurate. The vehicle stability constraints are expressed through the slip angles by

$$\alpha_f^{\rm min} \le \alpha_f \le \alpha_f^{\rm max}, \tag{11a}$$
$$\alpha_r^{\rm min} \le \alpha_r \le \alpha_r^{\rm max}, \tag{11b}$$

where $\alpha_f^{\rm max} = -\alpha_f^{\rm min}$, $\alpha_f^{\rm max} \le p_f$, $\alpha_r^{\rm max} = -\alpha_r^{\rm min}$, and $\alpha_r^{\rm max} \le p_r$.

Next we propose several constraints on the driver's feel divided into two groups, time-invariant formulations and reconfigurable formulations.

A. Driver's feel time-invariant constraints

We propose two time-invariant constraints on the driver's feel. The first one is related to the absolute feedback torque provided to the driver

$$T_{\rm fb}^{\rm min} \le T_{\rm fb} \le T_{\rm fb}^{\rm max}, \tag{12}$$

or after substituting $T_{\rm fb}$ by (9),

$$T_{\rm fb}^{\rm min} \le T_{\rm aln} - T_{\rm mot} \le T_{\rm fb}^{\rm max}, \tag{13}$$

where $T_{\rm fb}^{\rm min}$ [Nm] and $T_{\rm fb}^{\rm max}$ [Nm] are constant design values. Thus, (13) limits the total amount of torque provided to the driver independently of the driving conditions, i.e., independently of the actual alignment torque.

Another constraint is formulated in terms of the allowable intervention of the steering assist system with respect to the torque currently applied by the driver,

$$T_{\rm int}^{\rm min} \le T_{\rm drv} - T_{\rm mot} \le T_{\rm int}^{\rm max}, \tag{14}$$

where $T_{\rm int}^{\rm min}$ [Nm], $T_{\rm int}^{\rm max}$ [Nm] are constant bounds.

The driver's feel constraints (13) and (14) are relatively simple to implement, but rather limited. The time-invariant feel torque constraint (12) imposes the same limitation on the torque felt in all conditions, and as a consequence the torque provided by the motor may not be related to the driver's actions. In addition, the motor may be forced by the constraints to apply a torque and affect the steering feel even when not needed. For these reasons, we introduce reconfigurable constraints.

B. Driver's feel reconfigurable constraints

Reconfigurable constraints are modified according to the current vehicle and driver conditions. More specifically, three reconfigurable constraints on the driver's feel are investigated. The first constraint accounts for the feedback torque $T_{\rm fb}$,

$$\begin{cases} (1-c)T_{\rm aln} - \epsilon \le T_{\rm fb} \le (1+c)T_{\rm aln} + \epsilon & \text{if} \quad T_{\rm aln} \ge 0 \\ (1+c)T_{\rm aln} - \epsilon \le T_{\rm fb} \le (1-c)T_{\rm aln} + \epsilon & \text{if} \quad T_{\rm aln} < 0, \end{cases} \tag{15}$$

where $c \in (0,1)$, and $\epsilon > 0$ is a constant and small torque value, for instance 10% of the maximum driver torque. Constraint (15) can be written equivalently as

$$\begin{cases} -cT_{\rm aln} - \epsilon \le -T_{\rm mot} \le cT_{\rm aln} + \epsilon & \text{if} \quad T_{\rm aln} \ge 0 \\ cT_{\rm aln} - \epsilon \le -T_{\rm mot} \le -cT_{\rm aln} + \epsilon & \text{if} \quad T_{\rm aln} < 0\ . \end{cases}$$

Constraint (15) enforces the feedback torque to be in a region defined by the current alignment torque, and it changes with the sign of $T_{\rm aln}$, in order to guarantee feasibility, i.e., $T_{\rm mot} = 0$, can always be commanded.

Another constraint limits the maximum and minimum amount of torque that the driver can feel in relation to the torque that the driver is applying to the steering wheel,

$$\begin{cases} -\epsilon \le T_{\rm str} \le T_{\rm drv} + \epsilon & \text{if} \quad T_{\rm drv} \ge 0 \\ T_{\rm drv} - \epsilon \le T_{\rm str} \le \epsilon & \text{if} \quad T_{\rm drv} < 0, \end{cases} \tag{16}$$

where, as previously said, $T_{\rm str} = T_{\rm fb}$. Constraint (16) can also be formulated as

$$\begin{cases} -T_{\rm aln} - \epsilon \le -T_{\rm mot} \le T_{\rm drv}^{\rm fb} + \epsilon & \text{if} \quad T_{\rm drv} \ge 0 \\ T_{\rm drv}^{\rm fb} - \epsilon \le -T_{\rm mot} \le -T_{\rm aln} + \epsilon & \text{if} \quad T_{\rm drv} < 0, \end{cases}$$

where $\epsilon > 0$ is a small positive constant. Constraint (16) can be proved to be always feasible. Consider the case $T_{\rm drv} \ge 0$, then $T_{\rm aln} + T_{\rm drv}^{\rm fb} \ge 0$ and $T_{\rm aln} \ge -T_{\rm drv}^{\rm fb}$. Thus,

$$-T_{\rm aln} - \epsilon \le -T_{\rm aln} \le T_{\rm drv}^{\rm fb} \le T_{\rm drv}^{\rm fb} + \epsilon,$$

which shows that there always exist values of $T_{\rm mot}$ that satisfy (16). A similar procedure is followed for $T_{\rm drv} < 0$. Constraint (16) limits the steering assist system torque in

relation to the driver torque, but enough authority is left to the assist system to countersteer, if needed.

The third reconfigurable constraint is obtained as a combination (15) and (16),

$$\begin{cases} T_{\rm aln} - \epsilon \le T_{\rm str} \le T_{\rm drv} + \epsilon & \text{if} \quad T_{\rm drv} \ge T_{\rm aln} \\ T_{\rm drv} - \epsilon \le T_{\rm str} \le T_{\rm aln} + \epsilon & \text{if} \quad T_{\rm drv} < T_{\rm aln}, \end{cases} \tag{17}$$

which can be equivalently expressed as

$$\begin{cases} -\epsilon \le -T_{\rm mot} \le T_{\rm drv}^{\rm fb} + \epsilon & \text{if} \quad T_{\rm drv} \ge T_{\rm aln} \\ T_{\rm drv}^{\rm fb} - \epsilon \le -T_{\rm mot} \le \epsilon & \text{if} \quad T_{\rm drv} < T_{\rm aln}. \end{cases}$$

Next, we show how to design a control system for enforcing time-invariant and reconfigurable constraints. We design controllers based on model predictive control, due to its capability of handling complex constraints on system states and inputs, while compensating prediction model errors and external disturbances by feedback.

V. Control Design

The control objective is to track a desired vehicle yaw rate while satisfying the driver constraints, and at the same time preventing the vehicle from becoming unstable.

A. Prediction model

The MPC prediction model for control design is based on the steering and vehicle dynamics models developed in Section II, and on the driver model developed in Section III. The dynamics of the prediction model obtained by combining vehicle dynamics (4), steering dynamics (5), (6), and driver model (7), (8) are converted in discrete time with sampling period $t_s = 50$ ms. Thus, we have

$$x(k+1) = A^d x(k) + B^d u(k) + E^d w(k) \tag{18a}$$
$$y(k) = C^d x(k), \tag{18b}$$

where $x = [\alpha_f \ \alpha_r \ \delta \ \varphi]'$, $u = T_{\rm mot}$, $w = r_{\rm des}$, and $y = r$. The prediction model for the reference yaw rate can be generated in multiple ways [1]. In this paper we consider the desired yaw rate to be constant in prediction, i.e., for $h \in \mathbb{Z}_+$,

$$r_{\rm des}(h|k) = r_{\rm des}(k). \tag{19}$$

In order to impose constraints on the variation of the motor torque (10b), we define

$$T_{\rm mot}(k+1) = T_{\rm mot}(k) + \Delta T_{\rm mot}(k), \tag{20}$$

where $\Delta T_{\rm mot}^{\rm min} \le \Delta T_{\rm mot}(k) \le \Delta T_{\rm mot}^{\rm max}$, and $\Delta T_{\rm mot}^{\rm max} = -\Delta T_{\rm mot}^{\rm min} = t_s \dot{T}_{\rm mot}^{\rm max}$. By including as ancillary states the desired yaw rate $r_{\rm des}$ and the motor torque $T_{\rm mot}$, the MPC prediction model is obtained as

$$x_p(k+1) = A^p x_p(k) + B^p u_p(k), \tag{21a}$$
$$A^p = \left[\begin{smallmatrix} A^d & E^d & B^d \\ 0 & 1 & 0 \\ 0 & 0 & 1 \end{smallmatrix}\right], \ B^p = \left[\begin{smallmatrix} B^d \\ 0 \\ 1 \end{smallmatrix}\right], \tag{21b}$$

where the state vector of the augmented prediction model is $x_p = [\alpha_f \ \alpha_r \ \delta \ \varphi \ r_{\rm des} \ T_{\rm mot}]'$ and the control input is $u_p = \Delta T_{\rm mot}$, the rate of the motor torque.

B. Linear and switched MPC design

The MPC controller solves at every control cycle the finite horizon optimal control problem

$$\min_{U_N(k)} \quad \sum_{h=0}^{N-1} x_p(h|k)' Q x_p(h|k) + u_p(h|k)' R u_p(h|k) \tag{22a}$$
$$\text{s.t.} \quad x_p(h+1|k) = A^p x_p(h|k) + B^p u_p(h|k), \tag{22b}$$
$$z_p(k) = H^p x_p(h|k) + M^p u_p(h|k) \tag{22c}$$
$$u_{\min} \le u_p(h|k) \le u_{\max}, \ {\scriptstyle h=0,\dots,N_u-1} \tag{22d}$$
$$x_{\min} \le x_p(h|k) \le x_{\max}, \ {\scriptstyle h=1,\dots,N_c} \tag{22e}$$
$$z_{\min} \le z_p(h|k) \le z_{\max}, \ {\scriptstyle h=0,\dots,N_c-1} \tag{22f}$$
$$u_p(h|k) = 0, \ {\scriptstyle h=N_u,\dots,N-1} \tag{22g}$$

where $U_N(k) = (u_p(0|k), \dots, u_p(N-1|k))$. The prediction horizon N may be different from the constraint horizon N_c, the number of steps along which the state constraints are enforced, and from the control horizon N_u, the number of free control moves to be chosen. Besides (22d) and (22e), that enforce the constraints on the slip angles (11), the motor torque and the motor torque rate (10), the constraints related to driver's feedback (13), (14) are enforced by (22c), (22f) using the auxiliary vector z_p. In order to optimize tracking of the desired yaw rate, the cost function in (22a) implements

$$J = \ \sum_{k=0}^{N-1} q_r (r(h|k) - r_{des}(h|k))^2 + q_u u^2(h|k). \tag{23}$$

where $q_r, q_u > 0$ are cost function weights. At every cycle, the MPC controller solves (23) to obtain the optimal control sequence $U_N^*(k)$, and then applies to the steering assist system $T_{\rm mot}(k) = T_{\rm mot}(k-1) + u_p(k)$, where $u_p(k) = u_p^*(0|k)$.

The MPC scheme (22) cannot directly handle the reconfigurable constraints (15)–(17) due to their switching nature. In order to account for reconfigurable constraints we apply a switched Model Predictive Control (sMPC) strategy [15], where for any reconfigurable constraint two alternative sets of constraints on the auxiliary vector z_p are generated,

$$z_p(h|k) = H_{i(k)}^p x_p(h|k) + M_{i(k)}^p u_p(h|k), \tag{24a}$$
$$z_{\min}^{i(k)} \le z_p(h|k) \le z_{\max}^{i(k)}, \tag{24b}$$

where $i(k) \in \{1, 2\}$, for every $k \in \mathbb{Z}_{0+}$, thus resulting in two MPC problems. At control cycle k, the value of $i(k) = \bar{\imath}$, $\bar{\imath} \in \{1, 2\}$, is assigned by evaluating the switching condition for the current state (e.g., in (15), $T_{\rm drv} \ge 0$), and the MPC problem enforcing (24), for $i(k) = \bar{\imath}$, (e.g., $(1-c)T_{\rm aln} - \epsilon \le T_{\rm fb} \le (1+c)T_{\rm aln} + \epsilon$) along the whole constraints horizon is solved. The constraint switches are "frozen" during the prediction horizon, but they will be updated at the following control cycle according to the receding horizon nature of MPC. For more details on the switched MPC strategy, including stability results, the reader is referred to [15].

VI. Simulation Results

In the simulations we use the vehicle parameters from [15] that have been validated experimentally. In details we use

$m = 2050$ kg, $I_z = 3344$ kgm^2, $a = 1.43$ m, $b = 1.47$ m, and $v_x = 20$ m/s (72 km/h).

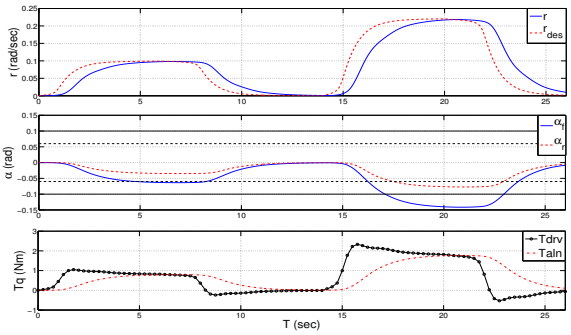

Fig. 3: Trajectories without controller.

The parameters of the linear tire forces region estimated from data in [15] are $c_f = -3.2 \cdot 10^4$ for the front tires, where the saturation angle is $p_f = 0.12$ rad, and $c_r = -5.7 \cdot 10^{-4}$ for the rear tires, with saturation angle $p_r = 0.07$ rad. The MPC controllers are implemented with $t_s = 50$ ms and horizons $N = 10$ for prediction, $N_u = 8$ for control, and $N_c = 7$ for constraints. The limits of the state and input ranges in (22) are $\alpha_{\rm f}^{\max} = -\alpha_{\rm f}^{\min} = 0.1$ rad, $\alpha_{\rm r}^{\max} = -\alpha_{\rm r}^{\min} = 0.06$ rad. $T_{\rm mot}^{\max} = -T_{\rm mot}^{\min} = 13.5$ Nm, $\Delta T_{\rm mot}^{\max} = -\Delta T_{\rm mot}^{\min} = 0.5$ Nm/t$_{\rm s}$, while $q_r = 10$, and $q_u = 0.1$. In order to maintain feasibility, the slip angles constraints (11) are enforced as soft constraints [17].

We have evaluated the performance in the simulation of four step steer maneuvers. In Figure 3 the trajectories when the control system is inactive ($T_{\rm mot}(k) = 0$ for all $k \in \mathbb{Z}_{0+}$) are shown. Obviously, $T_{\rm fb} = T_{\rm aln}$ but during the last two step steers the slip angles largely violate the stability constraints. Also, note that in the first step steer the settling time is close to 5s.

In Figure 4 we present the trajectories for the case where only mechanical constraints (10), (11) are enforced. In this case, the MPC controller clearly assists the driver in tracking the yaw rate reference trajectory during the first two step steers, hence improving the cornering performance (settling time is now close to $3s$) with respect to the uncontrolled case, Figure 3, while during the last two step steers it forces the slip angles to remain within the specified limits, hence guaranteeing vehicle stability. Nevertheless, the motor torque is large, and the steering feedback torque to the driver is significantly distorted (see Fig. 4(b)). In order to account for driver's feel as well, we introduce the constraints discussed in Section IV, and implement both mechanical and driver's feel constraints simultaneously.

In Figure 5 the results of implementing the fixed constraint (14) on the steering assist system intervention $T_{\rm drv} - T_{\rm mot}$ are presented. In the simulation, the limits, $T_{\rm int}^{\min}$ and $T_{\rm int}^{\max}$, are set to -2.5 Nm and 2.5 Nm, respectively. Thus, the control system has significant authority, i.e., the applied motor torque $T_{\rm mot}$ can assume large values. Figure 5 shows that the intervention of the steering assist system saturates the enforced constraints during the last two step steers.

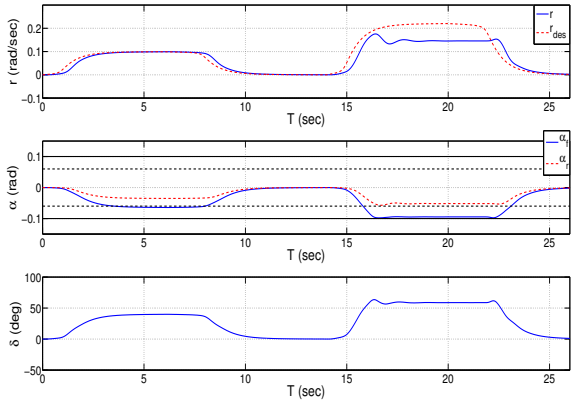

(a) Yaw rate, slip angles, steering wheel angle

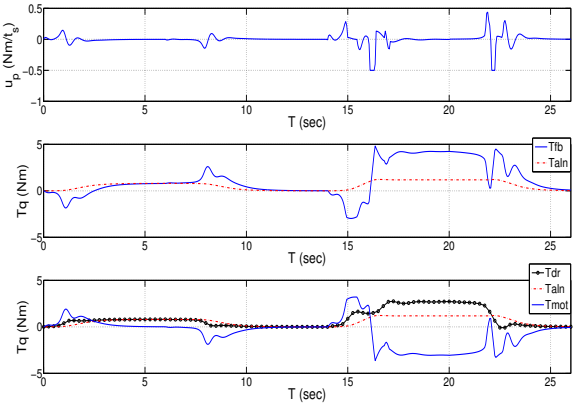

(b) Control input, feel torque, torques at steering wheel

Fig. 4: Trajectories without driver's feel constraints

Due to the aggressiveness of the maneuver, it is impossible to enforce both slip angles and driver torque constraints. Thus, the slip angles constraints are violated, and the vehicle state leaves the region where the linear model provides a good approximation of the vehicle dynamics. However, the constraint violation is significantly reduced with respect to the uncontrolled case (Figure 3). The driver's feel is affected less than in the previous case, but during the more aggressive maneuvers, the feedback torque to the driver is still significantly different from $T_{\rm aln}$.

In Figure 6 the effects of the combination of the maximum (minimum) allowed feel torque and strain torque (17) are shown, where $\epsilon = 0.2$ Nm. In this case the controller is able to keep the slip angles very close to the bounds during the last two step steers, although a small violation occurs. Moreover, the steering feedback torque to the driver $T_{\rm fb}$ in the first two step steers is almost identical to $T_{\rm aln}$. During the last two step steers it follows $T_{\rm aln}$ with a small, almost constant difference, except for the time period between 17 and 22(sec) during which the stability constraints are being enforced and $T_{\rm fb}$ deviates slightly more from $T_{\rm aln}$.

The simulation results in Figures 5–6 highlight the fun-

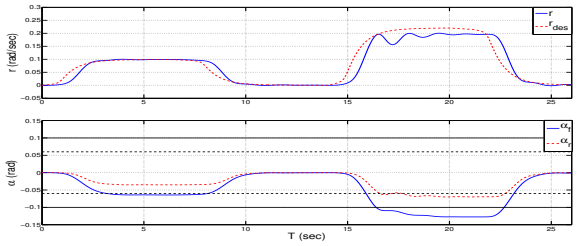

(a) Yaw rate, slip angles, steering wheel angle

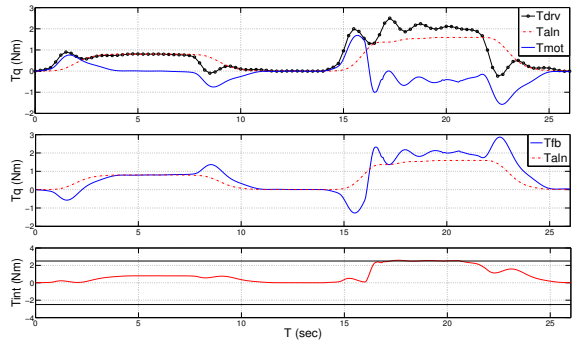

(b) Control input, feel torque, torques at steering wheel, motor intervention

Fig. 5: Trajectories with constraint on assist system intervention (14)

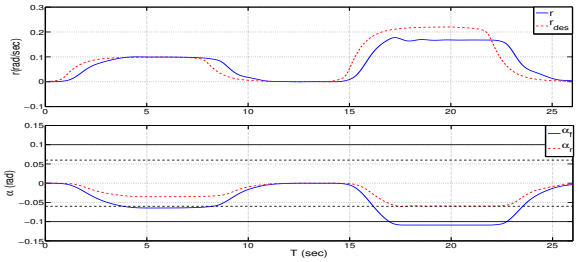

(a) Yaw rate, slip angles, steering wheel angle

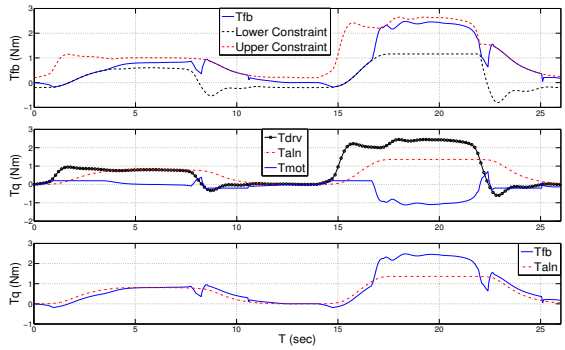

(b) Control input, feel torque, torques at steering wheel, feel torque and limits

Fig. 6: Trajectories with combined reconfigurable constraints (17)

damental trade-off between driver's feel (i.e., comfort) and vehicle control performance. The proposed strategy improves the yaw rate tracking performance compared to the uncontrolled case (Figure 3) and even when it is not possible to entirely meet the slip angles constraints (11), the controller minimizes the constraint violations (especially on α_r, which is the most critical angle for vehicle stability [15]) providing a significant improvement with respect to the uncontrolled case.

VII. Conclusions

In this paper we have introduced constraints that enforce driver's steering torque feel and we have presented the design and implementation of a steering assist system that improves vehicle cornering and stability, while enforcing the driver's feel constraints. Indeed, there is a fundamental trade-off between the distortion of the driver's feel and the vehicle control performance, and different constraints can be enforced to achieve the desired trade-off.

References

[1] H. Tseng, B. Ashrafi, D. Madau, T. Allen Brown, and D. Recker, "The development of vehicle stability control at Ford," *IEEE/ASME Tr. Mechatronics*, vol. 4, no. 3, pp. 223 –234, 1999.

[2] C. Farmer, "Effect of Electronic Stability Control on Automobile Crash Risk," *Traffic Injury Prevention*, vol. 5, no. 4, pp. 317–325, 2004.

[3] J. Ackermann, "Robust control prevents car skidding," *Control Systems Magazine*, vol. 17, no. 3, pp. 23 –31, 1997.

[4] B. Guvenc, T. Acarman, and L. Guvenc, "Coordination of steering and individual wheel braking actuated vehicle yaw stability control," in *IEEE Symp. Intell. Vehicles*, 2003, pp. 288 – 293.

[5] P. Falcone, F. Borrelli, J. Asgari, H. Tseng, and D. Hrovat, "Predictive active steering control for autonomous vehicle systems," *IEEE Tr. Contr. Systems Technology*, vol. 15, no. 3, pp. 566 –580, 2007.

[6] S. Di Cairano and H. Tseng, "Driver-assist steering by active front steering and differential braking: Design, implementation and experimental evaluation of a switched model predictive control approach," in *Proc. 49th IEEE Conf. on Dec. and Control*, 2010, pp. 2886 –2891.

[7] Y. Liao and H. Du, "Modelling and analysis of electric power steering system and its effect on vehicle dynamic behaviour," *Int. J. Vehicle Auton. Systems*, vol. 1, no. 2, pp. 153 – 166, 2003.

[8] Y. Hsu and J. Gerdes, "A feel for the road: A method to estimate tire parameters using steering torque," *Int. Sym. Adv. Vehicle Control*, 2006.

[9] R. Pastorino, M. A. Naya, J. A. Prez, and J. Cuadrado, "Geared pm coreless motor modelling for drivers force feedback in steer-by-wire systems," *Mechatronics*, vol. 21, no. 6, pp. 1043 – 1054, 2011.

[10] A. Zaremba, M. Liubakka, and R. Stuntz, "Control and steering feel issues in the design of an electric power steering system," in *Proc. American Contr. Conf.*, 1998, pp. 36 –40.

[11] Y. Morita, K. Torii, N. Tsuchida, M. Iwasaki, H. Ukai, N. Matsui, T. Hayashi, N. Ido, and H. Ishikawa, "Improvement of steering feel of electric power steering system with variable gear transmission system using decoupling control," in *10th IEEE Int. Work. Advanced Motion Control*, 2008, pp. 417 –422.

[12] C. E. Garcia, D. M. Prett, and M. Morari, "Model predictive control: Theory and practice - a survey," *Automatica*, vol. 25, no. 3, pp. 335 – 348, 1989.

[13] T. Gillespie, "Fundamentals of vehicle dynamics," *SAE*, 1992.

[14] H. Pacejka, *Tire and vehicle dynamics*. SAE, 2006.

[15] S. Di Cairano, H. Tseng, D. Bernandini, and A. Bemporad, "Vehicle yaw stability control by coordinated active front steering and differential braking in the tire sideslip angles domain," in *IEEE Tr. Contr. Systems Technology*, 2012, to appear.

[16] C. Ahn, H. Peng, and H. Tseng, "Robust estimation of road friction coefficient," in *Proc. American Contr. Conf.*, 2011, pp. 3948 –3953.

[17] S. Di Cairano, D. Yanakiev, A. Bemporad, I. Kolmanovsky, and D. Hrovat, "Model predictive idle speed control: Design, analysis, and experimental evaluation," *IEEE Trans. Contr. Systems Technology*, vol. 20, no. 1, pp. 84 –97, 2012.